Available online at www.sciencedirect.com

ScienceDirect

CAAI Transactions on Intelligence Technology 1 (2016) 285–292
http://www.journals.elsevier.com/caai-transactions-on-intelligence-technology/

Original Article

Manifold alignment using discrete surface Ricci flow

Zhongxin Liu [a], Wenmin Wang [a,*], Qun Jin [b]

[a] School of Electronic and Computer Engineering, Shenzhen Graduate School, Peking University, China
[b] Faculty of Human Sciences, Waseda University, Japan

Available online 19 October 2016

Abstract

Manifold alignment is useful to extract the shared latent structure among multiple data sets and the similarity among different datasets. As many kinds of real world data can be analyzed using low dimensional representations, manifold alignment algorithms can be used in a wide range of applications, such as data mining. In this paper, we propose a three-stage approach to manifold alignment using discrete surface Ricci flow. Our approach transforms the original intrinsic manifolds to hyper spheres using conformal mapping in the first stage, and then zooms these hyper spheres into the same scale and aligns them in the following stages. We describe in details about our algorithm, its theoretical principles, our experimental results, and the comparison to previous alignment methods. To prove the effectiveness of our algorithm, three kinds of experiments are presented, including a toy dataset, one containing parallel corpus of parliament proceedings and another containing both images and texts. With these experiments, the latent utility in discovering the similarity among different kinds of data sets can be demonstrated, whether within the same kind of data or across different kinds of modals of data.

Keywords: Cross-lingual retrieval; Cross-media retrieval; Dimensionality reduction; Manifold alignment

1. Introduction

With the increasing popularity of multimedia and the increasing volume of data, manifold alignment is helpful to extract the shared latent structure among multiple data sets, and to extract the similarity among different data sets. However, the features of different data sets may be disparate, which causes the difficulty to extract the correspondence in the original high dimensional space.

Manifold alignment algorithms are based on the mapping approaches which project high dimensional data into their latent low dimensional structures, such as manifold learning. The most widely used linear projection algorithms include principle component analysis (PCA) algorithm [29], isometric mapping (Isomap) algorithm [23], local linear embedding (LLE) [22], Laplacian Eigenmaps [1], locality preserving projections (LPP) algorithm [12], local tangent space alignment (LTSA) algorithm [35], adaptive manifold learning [36], Hessian Eigenmaps (HLLE) [6], hierarchical manifold learning algorithm [2] and inductive manifold learning [13].

On the basis of manifold learning algorithms which explore the latent low dimensional structure in a single data set, manifold alignment algorithms are useful to find the similarities of the latent low dimensional structures among different data sets.

A lot of manifold alignment algorithms have been proposed. Ham, Lee and Saul [10] aligned the manifolds leveraging a set of correspondences. Wang and Mahadevan [24] proposed a method based on Procrustes Analysis, which results in a mapping that is defined everywhere rather than just on the training data points. After then Wang and Mahadevan [27] described a framework that constructs functions mapping data instances from different high dimensional data sets to a new lower dimensional space, simultaneously matching the instances in correspondence and preserving pairwise distances between instances within the original data set. Li, Lv and Yi [15] provided an

* Corresponding author.
E-mail addresses: liuzhongxin1990@126.com (Z. Liu), wangwm@ece.pku.edu.cn (W. Wang), jin@waseda.jp (Q. Jin).
Peer review under responsibility of Chongqing University of Technology.

http://dx.doi.org/10.1016/j.trit.2016.10.002

algorithm to preserve the local geometry of the original data set, in which the sparse reconstruction weight matrix of each manifold is established by sparse manifold clustering and embedding (SMCE) method. Yang, Xu and Zhang [31] presented an alignment algorithm using local tangent space alignment. This algorithm can be helpful to keep the local structure in the neighborhood of the feature points. Wang and Mahadevan [26] proposed a general framework for the algorithms of manifold alignment. This framework combines three important viewpoints into manifold algorithms. The first one is the methods of probability, such as Procrustes Analysis, which is helpful to analysis the distribution of data. The next one is semi-supervised learning, which is widely used in data mining. The third one is semi-definite programming, which can provide a wider range of use than linear programming algorithms. Manifold alignment algorithms based on supervised learning [34], semi-supervised learning [14,30] and unsupervised learning [25] have been proposed as well. Wang and Mahadevan [28] proposed the multi-scale manifold algorithm, which can analyze the properties of data in multiple scales, using wavelet analysis.

As manifold alignment algorithms have attracted much attention, the application to real world problems, which process sparse high-dimensional data, has also been studied. Yang and Crawford [32] proposed an approach to combining alignment algorithms with remote sensing. This algorithm is designed to process multi-temporal hyper-spectral data.

However, there are still some problems to be solved. When the original high dimensionalities are relatively small and the volumes of data sets are quite large, it can be imagined that the surface of the manifolds are composed of numerous wrinkles. Consequently, it is difficult to construct a smooth function to describe the surfaces of these manifolds. To the contrary, when the original high dimensionalities are quite large and the volumes of data sets are relatively small, the data sets become extremely sparse. In this circumstance, it is nearly impossible to determine the structure of these manifolds. As described above, it is a big challenge to align these high dimensional data sets because of the irregular structure of their intrinsic low dimensional manifolds.

Although a lot of attention has also been paid to the research of deforming the irregular surfaces into flatten structures, the proposed methods can only be effective in restricted situations. For example, the Mobius Voting algorithm, proposed by Lipman and Funkhouser [16], is designed for three-dimensional spaces, rather than high dimensional spaces.

In this paper, we propose an approach based on discrete surface Ricci flow to solve the problems discussed above. In our approach, the original intrinsic manifolds of the data sets are transformed to hyper spheres via conformal mapping. The relative distances between each pair of data points on the surfaces are preserved, and then these hyper spheres are aligned. The generated manifolds are zoomed into the same scale, and then they are aligned to minimize the distance between each pair of corresponding points.

The rest of this paper is organized as follows. In Section 2, the theoretical background is presented. Section 3 gives a set of notations necessary to describe our manifold alignment algorithm. Section 4 shows the whole structure and the details of our manifold alignment algorithm based on discrete surface Ricci flow. Section 5 gives our analysis that proves the effectiveness of the proposed algorithm. Experimental results and discussions are given in Section 6. Finally, Section 7 provides concluding remarks.

2. Theoretical background

In this section, we briefly introduce the theoretical background of Riemannian metric and discrete surface Ricci flow.

Definition 1. (**Riemannian metric**). Suppose $\boldsymbol{S}$ is a surface, the Riemannian metric is a tensor $\boldsymbol{g} = (\boldsymbol{g_{ij}})$, which is positive definite, and defines an inner product for the tangent spaces of $\boldsymbol{S}$.

Definition 2. (**Gaussian curvature**). Let $\boldsymbol{S}$ be a surface with a Riemannian metric $\boldsymbol{g}$ and $(\boldsymbol{x}, \boldsymbol{y})$ be isothermal coordinates of $\boldsymbol{S}$, then the Gaussian curvature is defined as

$$k(x,y) = \Delta_g u(x,y) \tag{1}$$

where $\Delta \boldsymbol{g}$ is the Laplace–Beltrami operator induced by the original metric $\boldsymbol{g}$,.

Curvature is determined by the Riemannian metric and different metrics induce different curvatures. Both Gaussion curvature and the total curvature are widely used to measure the properties of surfaces. The total curvature is solely determined by the topology, as shown in Theorem 1. Riemannian metric in Teichmuller space is well defined and computable. Theoretic treatments can be found in [7].

Theorem 1. (**Gauss-Bonne**t) Let $(\boldsymbol{S}, \boldsymbol{g})$ be a metric surface, the total curvature is

$$\int_S K dA_g + \int_{\partial S} k_g ds = 2\pi\chi(S) \tag{2}$$

where $\boldsymbol{dA_g}$ is the element area of the surface, $\chi(S)$ is the Euler number of the surface, $\boldsymbol{K}$ is the Gaussian curvature, and k_g is the geodesic curvature.

Ricci flow is a powerful curvature flow method, invented by Hamilton [11] for the proof of the Poincareá conjecture [19,20,21]. Intuitively, it describes the process to deform the Riemannian metric according to curvature such that the curvature evolves like a heat diffusion process.The theoretic foundation for surface Ricci flow has been laid down for both smooth surfaces [4,11], and discrete meshes [5]. Surface Ricci flow and circle packing are discussed in detail in [8]. The theoretic results for inversive circle packing metric can be found in [9].

In our manifold alignment algorithm, surfaces are approximated by piecewise linear triangular meshes. In the following section, the smooth surface Ricci flow is generalized to the discrete setting.

Suppose $\boldsymbol{M}$ $(\boldsymbol{V}, \boldsymbol{E}, \boldsymbol{F})$ is a simplicial complex (triangle mesh) with vertex set $\boldsymbol{V}$, edge set $\boldsymbol{E}$, and face set $\boldsymbol{F}$,

respectively. The discrete Gaussian curvature is defined as angle deficient.

Definition 3. (**Discrete Gaussian curvature**) Suppose $\boldsymbol{M}$ is a mesh with a discrete metric, which is in Euclidean background geometry. $[\boldsymbol{v_i}, \boldsymbol{v_j}, \boldsymbol{v_k}]$ is a face in $\boldsymbol{M}$ and represents the corner angle at $\boldsymbol{v_i}$ on the face. The discrete Gaussian curvature of $\boldsymbol{v_i}$ is defined as

$$K_i = \begin{cases} 2\pi - \sum\limits_{jk} \theta_i^{jk}, v_i \notin \partial M \\ \pi - \sum\limits_{jk} \theta_i^{jk}, v_i \in \partial M \end{cases} \tag{3}$$

A circle packing associates each vertex with a circle. The circle at vertex $\boldsymbol{v_i}$ is denoted as $\boldsymbol{c_i}$. The two circles $\boldsymbol{c_i}$ and $\boldsymbol{c_j}$ on an edge $[\boldsymbol{v_i}, \boldsymbol{v_j}]$ are disjoint, or intersect each other at acute angle.

The generalized circle packing metric is defined as follows.

Definition 4. (**Generalized circle packing metric**) A generalized circle packing metric on a mesh $\boldsymbol{M}$ is to associate each vertex $\boldsymbol{v_i}$ with a circle $\boldsymbol{c_i}$, whose radius is $\boldsymbol{\gamma_i}$, associate each edge $[\boldsymbol{v_i}, \boldsymbol{v_j}]$ with a nonnegative number $\boldsymbol{I_{ij}}$. The edge length is given by

$$l_{ij} = \sqrt{\gamma_i^2 + \gamma_j^2 + 2I_{ij}\gamma_i\gamma_j} \tag{4}$$

The circle packing metric is denoted as $(\boldsymbol{\Gamma}, \boldsymbol{I}, \boldsymbol{M})$, where $\Gamma = \{\gamma_i\}$, $I = \{I_{ij}\}$. A discrete conformal deformation is to change radii $\boldsymbol{\gamma_i}$ s only, and preserve inverse distance $\boldsymbol{I_{ij}}$s. The discrete Ricci flow is defined as follows. Let us denote $\boldsymbol{u_i}$ as:

$$\boldsymbol{u_i} = \log \boldsymbol{\gamma_i} \tag{5}$$

Definition 5. (**Discrete Ricci flow**) Given a circle packing metric $(\boldsymbol{\Gamma}, \boldsymbol{I}, \boldsymbol{M})$, the discrete Ricci flow is

$$\frac{du_i}{dt} = \overline{K}_i - K_i \tag{6}$$

where $\overline{K}_i$ is the user-defined curvature at vertex $\boldsymbol{v_i}$.As discussed in the following theorem, high dimensional manifolds can also be mapped to hyper spheres.

Theorem 2. (**Brendle. S., Schoen. R.** [3]) Let $(\boldsymbol{M}, \boldsymbol{g})$ be an $\boldsymbol{n}$-dimensional compact Riemannian manifold with point-wise strictly 1/4-pinched curvature, where $\boldsymbol{n} \geq 4$, then $\boldsymbol{M}$ is diffeomorphic to a space sphere form.

3. Notations

3.1. Representation of the original data sets

$\boldsymbol{A} = [\boldsymbol{a_1}, \ldots, \boldsymbol{a_m}]$ is a matrix that is composed of $\boldsymbol{p}$ rows and $\boldsymbol{m}$ columns. In this matrix, $\boldsymbol{a_i}$ is determined by $\boldsymbol{p}$ features.

$\boldsymbol{B} = [\boldsymbol{b_1}, \ldots, \boldsymbol{b_n}]$ is another matrix that is composed of $\boldsymbol{q}$ rows and $\boldsymbol{n}$ columns. In this matrix, $\boldsymbol{b_i}$ is determined by $\boldsymbol{q}$ features.

Both $\boldsymbol{A}$ and $\boldsymbol{B}$ represent the original high-dimensional data set. The correspondences between $\boldsymbol{A}$ and $\boldsymbol{B}$ can be stated as follows. The data point $\boldsymbol{a_r}$ is related to $\boldsymbol{b_s}$, where $\boldsymbol{r}$ is an integer between $\boldsymbol{1}$ and $\boldsymbol{m}$, and $\boldsymbol{s}$ is an integer between $\boldsymbol{1}$ and $\boldsymbol{n}$.

3.2. Some necessary manifolds used in our algorithm

$\boldsymbol{A}^*$ and $\boldsymbol{B}^*$ represents the transformed manifolds related to $\boldsymbol{A}$ and $\boldsymbol{B}$, correspondingly. Both $\boldsymbol{A}^*$ and $\boldsymbol{B}^*$ can be considered as hyper spheres with the original high dimensionality, and they are necessary to construct the triangle meshes in our algorithm.

$\boldsymbol{A}'$ and $\boldsymbol{B}'$ represent the processed manifolds related to $\boldsymbol{A}$ and $\boldsymbol{B}$ correspondingly. These two manifolds denote the triangle meshes for manifold $\boldsymbol{A}$ and $\boldsymbol{B}$.

$\boldsymbol{A}''$ and $\boldsymbol{B}''$ are the reshaped manifolds that are deformed using discrete surface Ricci flow from manifold $\boldsymbol{A}'$ and $\boldsymbol{B}'$.

The correspondence between $\boldsymbol{A}''$ and $\boldsymbol{B}''$ is the same as that between $\boldsymbol{A}$ and $\boldsymbol{B}$. All of the manifolds mentioned above are shown in Fig. 1.

4. Our alignment algorithm

In this section, we propose an alignment algorithm, which is composed of three stages, i.e., the conformal transformation stage, the scale adjusting stage, and the alignment stage. As the surface structures of manifolds are quite complex, it can be too difficult to find a proper function to describe its shape exactly. Therefore, we intend to transform the original intrinsic manifolds in the first stage, after which they can be assumed to approximate hyper spheres. Then in the following stages, it is the hyper spheres that are to be adjusted and aligned, rather than

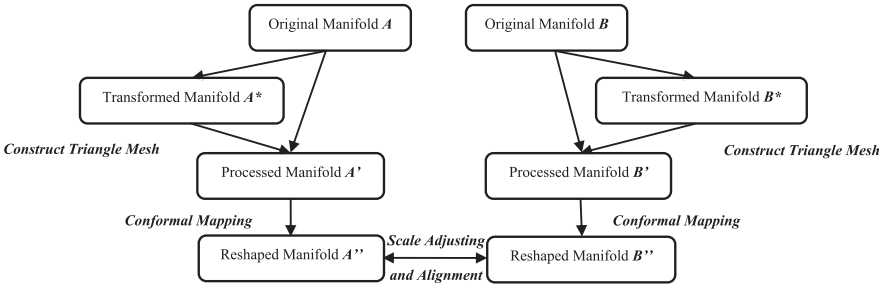

Fig. 1. Workflow of our alignment algorithm.

the original manifolds. This alignment process can be easier to implement because of the simplicity of surfaces.

The workflow of our alignment algorithm is shown in Fig. 1, in which the meanings for the symbols A, B, A^*, B^*, A', B', A'' and B'' have been described in the previous section.

Algorithm 1. Conformal Mapping Using Ricci Flow

Step 1. Compute edge lengths l_{ij} from the current vertex radii γ_i, γ_j and the fixed edge weight ϕ_{ij} using the cosine law for the background geometry, where:

$$\gamma_i^{jk} = \frac{l_{ki} + l_{ij} - l_{jk}}{2} \quad \gamma_i = \frac{1}{m} \sum_{f_{ijk} \in F} \gamma_i^{jk}$$
$$l_{ij}^2 = \gamma_i^2 + \gamma_j^2 + 2\gamma_i \gamma_j \cos\phi_{ij} \tag{7}$$

Step 2. Compute the corner angles θ_i^{jk} in each face f_{ijk} from the current edge lengths by using the cosine law according to the background geometry.

Step 3. Compute the discrete Gaussian curvature K_i of each vertex v_i, using (3).

Step 4. Update u_i of each vertex v_i as follows:

$$u_i = u_i + \varepsilon_i \times \left(\overline{K_i} - K_i\right) \tag{8}$$

where $\overline{K_i}$ is the target Gaussian curvature.

Step 5. Normalize the metrics. Let $s = \sum u_i$, then

$$u_i = u_i - \frac{s}{n} \tag{9}$$

where n is the total number of vertices.

Step 6. Update the radius γ_i of each vertex v_i, using (5).

Step 7. Repeat the steps from 1 through 6 until the maximal curvature error falls below a threshold data (it is set to be 0.01 in our experiments).

4.1. Stage 1: triangulation and conformal transformation stage

In this stage, we aim to transform the original manifolds to hyper spheres. As we intend to convert the problem of aligning two manifolds with complex structures to the problem of aligning two hyper spheres, it is important to preserve the structure features on the manifolds. We preserve the local structures on the manifolds in this stage. In other words, the relative distances between each data point with the data points in its neighborhood and the intersection angles formed by the edges connected to each data point are preserved. The preservation is of great help when aligning these hyper spheres.

This stage can be divided into three steps. In the first step, the original manifolds A and B are transformed to A^* and B^*, which are two hyper spheres having the same dimensionality with A and B. We calculate the centroid $\overline{a}$ of the manifold A, and transform each data point on A so that the distance between each data point a_c is the same as the largest one. This generated manifold is A^*. A^* is a hyper sphere with radius r and $\overline{a}$ means the centroid of manifold A. The correspondence between B and B^* is similar.

$$r = \max_{1 \le i \le p} \|a_i - \overline{a}\| \quad \overline{a} = \frac{1}{p} \times \sum_{1 \le i \le p} a_i \tag{10}$$

In the second step, we estimate the triangle meshes of A and B, with the help of A^* and B^*. For each pair of data point a_i and a_j from manifold A, denote their corresponding points on A^* as a_i^* and a_j^*. If the distance between a_i^* and a_j^* on A^* is greater than a threshold, a_i and a_j are considered to be disconnected on A. The manifold generated by strengthening manifold A with this relationship is the manifold A' described above. The relationship between B and B' is similar.

In the third step, we deform the manifolds A' and B' using Ricci flow. The generated manifolds are A'' and B'' correspondingly. The algorithm involved in the third step is described in Algorithm 1. The manifolds A'' and B'' are ready to be used in the alignment process.

4.2. Stage 2: scale adjusting stage

In this stage, we zoom the generated manifolds A'' and B'' into the same scale. In order to accomplish it, we adjust the coordinates on A'' so that it can be zoomed into the same scale as manifold B''. The scaling factor is related to the radius of the intermediate manifolds A^* and B^*, which are exactly hyper spheres.

Let the radius of A^* and B^* be r_A and r_B. Then we transfer the original manifolds A' and B' to the same scale, according to the ratio of r_A and r_B, as shown in the following equation.

$$a_i'' = \frac{r_B}{r_A} \times a_i'' \tag{11}$$

As depicted in Equation (11), if the intermediate manifolds A^* and B^* has the same radius, we consider the generated manifolds A'' and B'' to be in the same scale.

Then in the next stage, the adjusted manifolds A'' and B'' will be used to alignment.

4.3. Stage 3: alignment stage

In this stage, we align the hyper spheres obtained in the previous stage. As the structure of hyper spheres are easier to recognize than the original manifolds, we can rotate the hyper spheres to let the labeled data points be as close to each other as possible in the original high dimensional space.

Then these hyper spheres are mapped to low dimensional spaces, we perform this mapping with a Laplacian Eigenmaps algorithm. We can calculate the low dimensional coordinate for each data point and for each unlabeled data point, the most appropriate matching data point is assumed to be the nearest point on the other manifold. Let A''_{low} and B''_{low} represent the low dimensional representations of A'' and B''. In the low

dimensional space, an orthonormal matrix P is to be determined, which minimizes the Frobenius norm $\left\|A''_{low} - B''_{low}P\right\|$. The details of this stage are shown in Algorithm 2.

Algorithm 2. Alignment in Low Dimensionality

Step 1. Transform the coordinates of the matrices ***A''low*** *and* ***B''low***, so that their centroids are both at the same position after translation. Let the original coordinate of their centroids be the average of their data points, as shown in Equations (12) and (10).

$$center\left(A''_{low}\right) = \overline{A}_{low} = \frac{\sum_i \left(A''_{low}\right)_i}{\left|A''_{low}\right|} \tag{12}$$

$$center\left(B''_{low}\right) = \overline{B}_{low} = \frac{\sum_i \left(B''_{low}\right)_i}{\left|B''_{low}\right|} \tag{13}$$

Step 2. Calculate the SVD decomposition of the matrix $(B''_{low})^T A''_{low}$, as shown in Equation (14).

$$U\sum V = SVD\left(\left(B''_{low}\right)^T A''_{low}\right) \tag{14}$$

Step 3. The matrix $P = UV^T$ is expected.

5. Theoretical analysis

As mentioned above, in our algorithm, we transform the manifolds $\boldsymbol{A}$ and $\boldsymbol{B}$ into hyper spheres in the first step. The distances between each pair of points on these hyper spheres are used to determine the connectivity of points on $\boldsymbol{A}$ and $\boldsymbol{B}$. Therefore, it is of great significance to guarantee that the transformation preserves properties regards to connectivity on $\boldsymbol{A}$ and $\boldsymbol{B}$. In this section, we analyze this problem and state it as the following theorem.

Theorem 3. Let $\boldsymbol{a_i}$ and $\boldsymbol{a_j}$ be two points on manifold $\boldsymbol{A}$. Denote their corresponding points on manifold $A*$ as and $\boldsymbol{a_i^* a_j^*}$. If $\boldsymbol{a_i}$ and $\boldsymbol{a_j}$ are connected directly on manifold $\boldsymbol{A}$, then it is impossible to find an integer $\boldsymbol{k}$, $1 \le k \le m$, such that for some scalar λ and μ, $\boldsymbol{a_i^*}$, $\boldsymbol{a_j^*}$ and $\boldsymbol{a_k^*}$ satisfies Equation (15). In the equation, $\boldsymbol{a_{it}^*}$ means the $\boldsymbol{t}$-th coordinate of point $\boldsymbol{a_i^*}$, with

$$1 \le t \le p,\ 0 \le \lambda_1, \lambda_2 \le 1,\ 0 \le \mu \le 1,\ \lambda_1 + \lambda_2 = 1.$$
$$\lambda_1\left(a^*_{it} - \overline{a}\right) + \lambda_2\left(a^*_{jt} - \overline{a}\right) = \mu\left(a^*_{kt} - \overline{a}\right) \tag{15}$$

Proof. We prove this theorem by contradiction. First assume there exists $\boldsymbol{k}$, λ and μ that satisfies Equation (15) mentioned above. With the correspondence between manifolds $\boldsymbol{A}$ and $\boldsymbol{A}*$, we can get the following equations.

$$\begin{aligned} a^*_{it} &= \frac{r}{\|a_i - \overline{a}\|} \times (a_{it} - \overline{a}) + \overline{a}_t \\ a^*_{jt} &= \frac{r}{\left\|a_j - \overline{a}\right\|} \times \left(a_{jt} - \overline{a}\right) + \overline{a}_t \\ a^*_{kt} &= \frac{r}{\|a_k - \overline{a}\|} \times (a_{kt} - \overline{a}) + \overline{a}_t \end{aligned} \tag{16}$$

In these equations, $\boldsymbol{r}$ means the radius of hyper sphere $\boldsymbol{A}*$ and $\overline{a}$ means the centroid of manifold $\boldsymbol{A}$.

$$r = \max_{1 \le i \le p} \|a_i - \overline{a}\| \quad \overline{a} = \frac{1}{p} \times \sum_{1 \le i \le p} a_i \tag{17}$$

By substituting them into Equation (15), we can find that there exist $0 \le \lambda_1, \lambda_2 \le 1,\ 0 \le \mu \le 1,\ \ \lambda_1 + \lambda_2 = 1$ that satisfies the following equation.

$$\lambda_1 \times \frac{r}{\|a_i - \overline{a}\|} + \lambda_2 \times \frac{r}{\left\|a_j - \overline{a}\right\|} = \mu \times \frac{r}{\|a_k - \overline{a}\|} \tag{18}$$

Therefore, in this circumstance, it is reasonable to assume $\boldsymbol{a_i}$ and $\boldsymbol{a_k}$ to be connected directly. The point $\boldsymbol{a_j}$ and $\boldsymbol{a_k}$ can be assumed connected as well. While $\boldsymbol{a_i}$ and $\boldsymbol{a_j}$ are connected via $\boldsymbol{a_k}$, rather than directly.

$$\frac{\lambda_1 r}{\|a_i - \overline{a}\|} \times a_{it} + \frac{\lambda_2 r}{\left\|a_j - \overline{a}\right\|} \times a_{jt} = \frac{\mu r}{\|a_k - \overline{a}\|} \times a_{kt} \tag{19}$$

Our theorem is proven.

6. Experimental results

To test the effectiveness of our alignment algorithm, we use three data sets. The first one is Protein, which is a small data set. The second one is the European Corpus, which is a large data set used for cross-lingual retrieval. The third one is the Wikipedia's featured articles, which is used for cross-media retrieval. Both toy data set, which is easy to be drawn directly, and real world data sets, which are more complex, are used in our experiment. The experimental results using these data sets are discussed below.

6.1. Protein

It is well known that protein 3D structure reconstruction is useful for Nuclear Magnetic Resonance (NMR) protein structure determination. It can learn a map from distances to coordinates. NMR techniques can learn multiple models, rather than a single structure. The models which are related to the same protein should be similar.

Therefore, comparison between these models in the results can tell whether the NMR technique can determine protein conformation well.

In this part of experiment, we study the Glutaredoxin protein PDB-1G7O. This protein is composed of 215 amino acids in total and its three-dimensional structure has 21 models. Two of these models are selected for testing. Model 1 is denoted as the original manifold **A**, and model 2 is denoted as the original manifold **B**. These original manifolds are shown in Fig. 2 (A).

In order to align these two manifolds, we select 1/10 amino acids uniformly. Therefore, the number of labeled data points on each manifold is 22, which are known to be matched. Other 193 data points are assumed to be unlabeled, and they are used for testing.

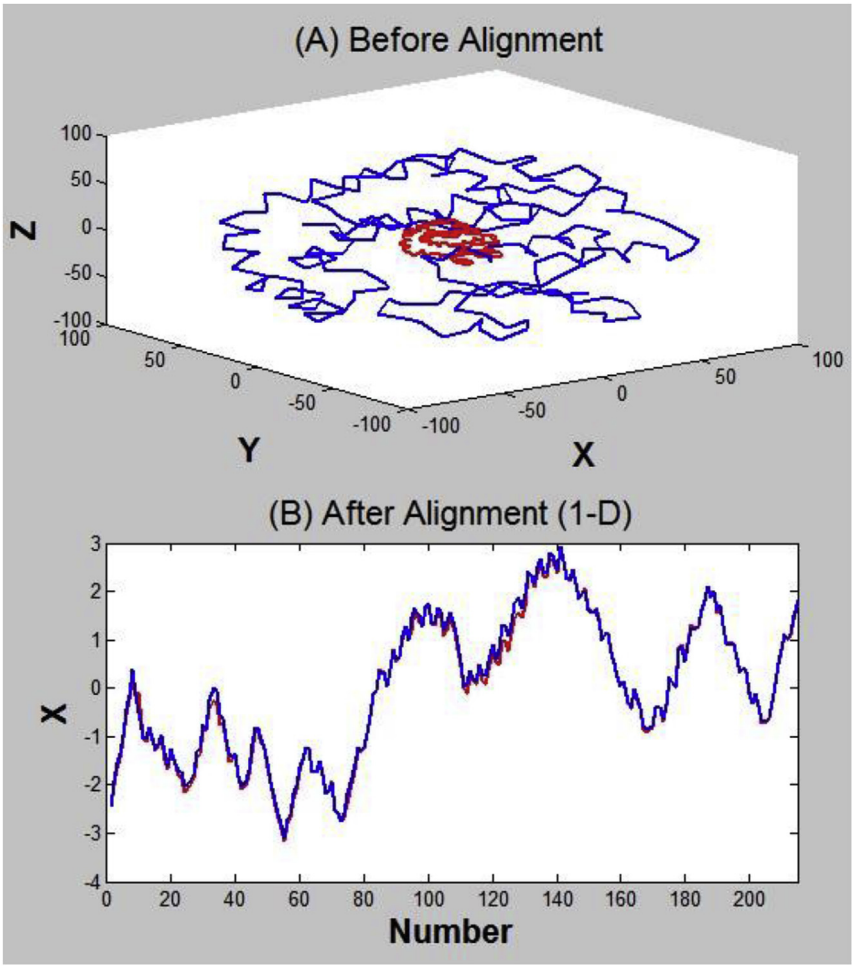

Fig. 2. Alignment results using protein dataset.

As shown in Fig. 2 (B), the low dimensional representation shows that our algorithm can align these manifolds well.

6.2. Cross-lingual retrieval

In this part of experiment, we use the data set of European Parliament Proceeding Parallel Corpus (Europarl Corpus), which contains the data from the year 1996–2011. This corpus is composed of numerous kinds of language, we select the parallel corpus of English and Italian, and extract the documents that contains more than 90 words. There are 2500 pairs of documents that satisfy this condition, each English document is represented by the most commonly used 1000 English words, and each Italian document is also represented by the

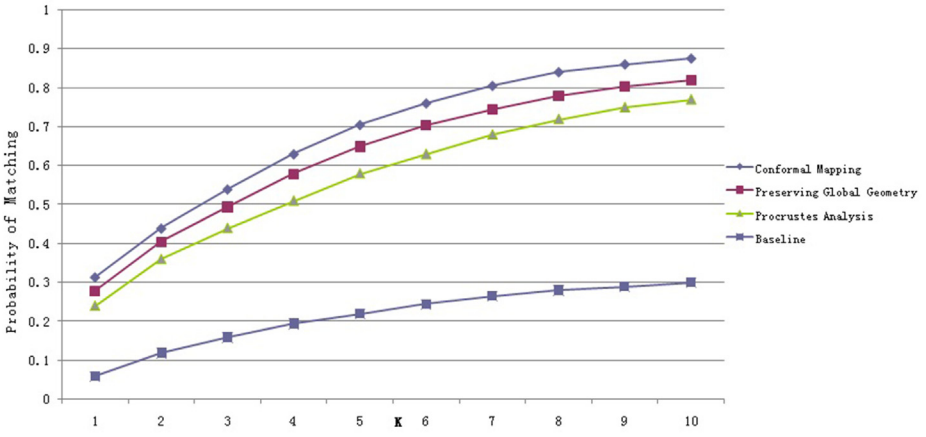

Fig. 3. Test on Europarl Corpus Dataset (20% instances are in the given correspondence).

most commonly used 1000 Italian words. Therefore, these original data points can be considered to come from a 1000 dimensional space.

We select other three typical algorithms for comparison: first one is the Procrustes alignment algorithm using LPP (Locality Preserving Projections), second one is the alignment algorithm preserving global geometry, and third one is the baseline algorithm. The baseline algorithm can be stated as follows.

Assume that there are n correspondences in the training data set, then the document x can be represented by a vector $\boldsymbol{V}$ whose length is $\boldsymbol{n}$. In this vector, $\boldsymbol{V(i)}$ represents the similarity between $\boldsymbol{x}$ and the $\boldsymbol{i}$-th document in the training correspondences. The baseline algorithm maps the documents from different collections into the same embedding space $\boldsymbol{R^n}$.

The effectiveness of alignment algorithms can be described as follows. For each English document, we select $\boldsymbol{k}$ Italian documents that are most similar with it. The effectiveness of these algorithms is represented by the probability for the true match to be among these $\boldsymbol{k}$ most similar documents. All of these algorithms map the data into a 100 dimensional space.

The accuracy of our algorithm is shown in Fig. 3. As shown in this figure, our algorithm Conformal Mapping can perform well using the Europarl Corpus data set.

6.3. Cross-media retrieval

In this experiment, we rely on Wikipedia's featured articles. This is a continually updated collection of articles that have been selected and reviewed by Wikipedia's editors. The articles are accompanied by one or more pictures from the Wikimedia Commons, supplying a pairing of the desired kind. In addition, each featured article is categorized by Wikipedia into one of 29 categories. These category labels were assigned to both the text and image components of each article. Since some of the categories are very scarce, we considered only the 10 most populated ones.

Each article was split into sections, based on its section headings, and each image in the article assigned to the section in which it was placed by the article author. This produced a set of short and focused articles, usually containing a single image. The dataset was finally pruned by removing the sections without any image. The final corpus contains a total of 2866 documents. A random split was used to produce a training set of 2173 documents, and a test set of 693 documents, as shown in Table 1.

Table 1
Summary of the dataset of Wikipedia featured articles.

Category	Training	Query/Retrieval	Total
Art & Architecture	138	34	172
Biology	272	88	360
Geography & Places	244	96	340
History	248	85	333
Literature & Theatre	202	65	267
Media	178	58	236
Music	186	51	237
Royalty & Nobility	144	41	185
Sport & Recreation	214	71	285
Warfare	347	104	451
Total	2173	693	2866

Table 2
Retrieval performance of the experiments.

Experiments	MAP (Image Query)	MAP (Text Query)	MAP (Average)
Random	0.118	0.118	0.118
Semi-definite Alignment	0.262	0.225	0.243
PFAR	0.298	0.273	0.286
LRGA	0.312	0.181	0.247
TSC-test	0.295	0.207	0.251
TSC-image	0.322	0.251	0.287
Our Method	**0.376**	**0.234**	**0.305**

To prove the effectiveness of our algorithm under the situation of cross-media retrieval, we selected different kinds of algorithms to compare with ours, including the random selection, the semi-definite manifold alignment algorithm [28], the parallel field alignment retrieval (PFAR) algorithm [18], the local regression and global alignment (LRGA) algorithm [33] and the temporal-spatial clustering (TSC) algorithm for text and image [17].

These selected algorithms can cover most of the widely used methods, such as linear/nonlinear algorithms, regression algorithms and manifold alignment algorithms. Among the above mentioned algorithm, the algorithms of LRGA and TSC can be considered as applications of manifold alignment algorithm to solve the problem of cross-media retrieval. Comparing with these algorithms, the effectiveness of processing the correspondence between images and texts using our algorithm can be proven.

The experimental results are show in Table 2. We use the MAP value as a criterion to evaluate these algorithms. It can be seen from the results that our algorithm can perform well on the problem of cross-media retrieval.

7. Conclusion

In this paper, we have proposed a manifold alignment algorithm using discrete surface Ricci flow, in order to transform a surface with a complex structure into a hyper sphere and then align these hyper spheres. The experimental results show that our algorithm can perform well on both small and large data sets. The alignment algorithm can not only explore the similarity of data of the same kind, but also can help find the similarity among different kinds of data.

In order to align two manifolds with complex structures, one of the most critical steps is constructing the triangle meshes to approximate intrinsic manifolds. However, when the intrinsic dimensionalities of manifolds are quite high, there may be more than one proper approach to construct the triangle meshes. Therefore, for future works, we will focus on searching for the approach to construct the most proper triangle meshes, which can both be efficient and approximate the manifold accurately, when the intrinsic structure is complex.

As is well known, the approximation of a surface includes two kinds of important aspects, i.e., the approximation of position and normal bundle. These two aspects are of much

significance in manifold alignment algorithms as well. The calculation of correspondences among different data sets can be regarded as the alignment of position in high dimensional spaces. However, alignment of the normal bundle among the latent manifolds can be helpful to understand the properties of data sets, such as semantic information.

As the semantic information of images or texts has attracted a lot of attention, the alignment algorithms among different kinds of data have faced with challenges because of semantic gap. For example, problems such as the relation between the singularity of geometrical structure on the low dimensional manifold of images and the difference of meaning of an image to all the other, may be meaningful to study.

References

[1] M. Belkin, P. Niyogi, Neural Comput. (2003) 1373–1396.
[2] K.K. Bhatia, et al., Med. Image Comput. Comput. Assist. Interv. (2012) 512–519.
[3] S. Brendle, R. Schoen, Acta Math. 200 (2008) 1–13.
[4] B. Chow, J. Differ. Geom. 33 (2) (1991) 325–334.
[5] B. Chow, F. Luo, J. Differ. Geom. 63 (1) (2003) 97–129.
[6] D.L. Donoho, C. Grimes, Locally linear embedding techniques for high-dimensional data, in: Proceedings of the National Academy of Sciences of the United States of America, 2003, pp. 5591–5596.
[7] F.P. Gardiner, N. Lakic, Am. Math. Soc. (2000). Technical Report, Nov. 5.
[8] X. Gu, S. Wang, J. Kim, Y. Zeng, Y. Wang, H. Qin, D. Samaras, in: Proceedings of the IEEE International Conference on Computer Vision, 2007.
[9] R. Guo, Local Rigidity of Inversive Distance Circle Packing, 2009 arXiv: 0903.1401v2.
[10] J. Ham, D. Lee, L. Saul, Annu. Conf. Uncertain. Artif. Intell. 10 (2005) 120–127.
[11] R.S. Hamilton, Math. General Relativ. 71 (1988) 237–262.
[12] X.F. He, P. Niyogi, Adv. Neural Inf. Process. Syst. (2004) 153–160.
[13] K. Kim, D. Lee, Pattern Recognit. (2014) 470–479.
[14] R. Jia, J. Electr. Eng. 12 (4) (2014).
[15] X. Li, C.J. Lv, Z. Yi, Manifold alignment based on sparse local structures of more corresponding pairs, in: Proceedings of the Twenty-third International Joint Conference on Artificial Intelligence, AAAI Press, 2013.
[16] Y. Lipman, T. Funkhouser, ACM 28 (3) (2009) 72.
[17] Y. Liu, et al., Cross retrieval method based on temporal-spatial clustering and Multimodal Fusion, in: Proceedings of the Fourth International Conference on the Internet Computing for Science and Engineering, 2009, pp. 78–84.
[18] X.B. Mao, et al., Parallel field alignment for cross media retrieval, in: Proceedings of the Twenty-first ACM International Conference on Multimedia, 2013, pp. 897–906.
[19] G. Perelman, The Entropy Formula for the Ricci Flow and its Geometric Applications, 2002 technical report, arXiv.org.
[20] G. Perelman, Ricci Flow with Surgery on Three-manifolds, 2003 technical report, arXiv.org.
[21] G. Perelman, Finite Extinction Time for the Solutions to the Ricci Flow on Certain Three-manifolds, 2003 technical report, arXiv.org.
[22] S.T. Roweis, L.K. Saul, Science (2000), pp. 2323-+.
[23] J.B. Tenenbaum, V. de Silva, J.C. Langford, Science (2000), pp. 2319-+.
[24] C. Wang, S. Mahadevan, Manifold alignment using Procrustes analysis, in: Proceedings of the 25th International Conference on Machine Learning, ACM, 2008, pp. 1120–1127.
[25] C. Wang, S. Mahadevan, Int. Jt. Conf. Artif. Intell. 38 (4) (2009) 1273–1278.
[26] C. Wang, S. Mahadevan, AAAI Fall Symposium (2009) 79–86.
[27] C. Wang, S. Mahadevan, Manifold alignment preserving global geometry, in: Proceedings of the Twenty-seventh International Joint Conference on Artificial Intelligencem, AAAI Press, 2013, pp. 1743–1749.
[28] C. Wang, S. Mahadevan, Multiscale Manifold Alignment, Technical Report, University of Massachusetts, 2010.
[29] S. Wold, K. Esbensen, P. Geladi, Chemom. Intelligent Laboratory Syst. (1987) 37–52.
[30] L. Xiong, F. Wang, C. Zhang, "Semi-definite Manifold Alignment", Machine Learning: ECML 2007, Springer Berlin Heidelberg, 2007, pp. 773–781.
[31] G.L. Yang, X. Xu, J.M. Zhang, Mainifold Alignment via local tangent space alignment, in: International Conference on Computer Science and Software Engineering, 2008, pp. 928–931.
[32] H.L. Yang, M.M. Crawford, Hyper Image Signal Process. Evol. Remote Sens. (2011) 1–4.
[33] Y. Yang, et al., Ranking with local regression and global alignment for cross media retrieval, in: Proceedings of the 17th ACM International Conference on Multimedia, 2009, pp. 175–184.
[34] D. Zhai, H. Chang, S. Shan, et al., in: British Machine Vision Conference, 2010, pp. 1–11.
[35] Z.Y. Zhang, H.Y. Zha, J. Shanghai Univ. Engl. Ed. (2004) 406–424.
[36] Z.Y. Zhang, J. Wang, H.Y. Zha, in: IEEE Trans. Pattern Anal. Mach. Intell., 2012, pp. pp.253–265.

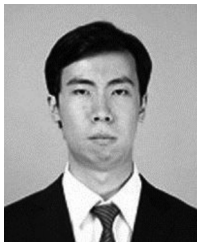

Zhongxin Liu received the B.S. degree in software engineering from Nankai University, Tianjin, China in 2012 and the M.S. degree in computer application technology from Peking University, Beijing, China in 2015. Since 2015, he has been a Software Engineer with the Baidu Co., Ltd, Beijing, China. His research interests include recommender systems, information retrieval, machine learning, computer vision, image processing, robotics and multi-agent systems.

Wenmin Wang received the Ph.D. degree in computer architecture from the Harbin Institute of Technology, Harbin, China, in 1989. After completing the Ph.D. degree, he was an Assistant Professor and an Associate Professor at the Harbin University of Science and Technology, Harbin, China, as well as the Harbin Institute of Technology. Since 1992, he gained about 18 years of oversea industrial experiences in Japan and America, in where served as a Staff Engineer, Chief Engineer, General Manager of Software Division, etc., for various companies. In 2009, he became a Professor at the School of Electronic and Computer Engineering, Peking University, Shenzhen, China. His current research interests include computer vision, multimedia retrieval, artificial intelligence, and machine learning.

Qun Jin is currently a tenured full professor at the Department of Human Informatics and Cognitive Sciences, Faculty of Human Sciences, Waseda University, Japan. He has been engaged extensively in research works in the fields of computer science, information systems, and social and human informatics. He seeks to exploit the rich interdependence between theory and practice in his work with interdisciplinary and integrated approaches. Dr. Jin has published more than 200 refereed papers in the world-renowned academic journals and international conference proceedings in the related research areas. His recent research interests cover human-centric ubiquitous computing, behavior and cognitive informatics, data analytics and big data security, personal analytics and individual modeling, cyber-enabled applications in e-learning and e-health, and computing for well-being. He is a member of IEEE, IEEE CS, and ACM, USA, IEICE, IPSJ, and JSAI, Japan, and CCF, China.